

Tuning the thermal conductivity of polymers with mechanical strains

Jun Liu and Ronggui Yang*

Department of Mechanical Engineering, University of Colorado, Boulder, Colorado 80309, USA

(Received 8 January 2010; revised manuscript received 12 April 2010; published 28 May 2010)

The low thermal conductivity of polymers limits their heat spreading capability, which is one of the major technical barriers for the polymer-based products, especially electronics, such as organic light emitting diodes. It is highly desirable to enhance the thermal conductivity of polymer materials including polymer composites. Mechanical stretching could align polymer chains which are intrinsically low-dimensional material that could have very high thermal conductivity and thus enhancing the thermal conductivity of polymers. In this work, the all-atom model molecular-dynamics simulation is conducted to investigate the tuning of polymer thermal conductivity using mechanical strains. The simulation results show that the thermal conductivity of polymers increases with the increasing strain and the enhancement is larger when the polymer is stretched slower. Molecular weight also affects the thermal conductivity under the same stretching condition. More importantly, the thermal-conductivity enhancement could be exponentially fitted with the orientational order parameter which describes the chain conformation change. This study could guide the development of advanced reconfigurable and tunable thermal management technologies.

DOI: [10.1103/PhysRevB.81.174122](https://doi.org/10.1103/PhysRevB.81.174122)

PACS number(s): 65.60.+a, 66.70.Hk, 68.35.bm

I. INTRODUCTION

Polymers have been widely used in many fields as functional or structural materials.^{1,2} There are also significant and new applications of polymers in macroelectronics such as large-scale organic display panels,³ solar panels,⁴ and batteries.⁵ The thermal conductivity of polymers are of great importance for many of these applications because they govern the temperature-rise magnitude and temporal thermal behavior of polymer-based products.⁶ However, polymers typically have very low thermal conductivity of 0.1–1 W/mK at room temperature⁷ which is two to three orders of magnitude lower than inorganic semiconductors and metals and thus greatly limiting the heat spreading capability of polymers. Engineering the thermal conductivity of polymer-based materials including thermal interface materials, shape memory polymers, and conductive polymers for electronics are of great technical importance but remains a big challenge although some progresses have been made.

Experimental and theoretical analyses have been employed in the past to study the heat conducting mechanisms in polymers. It has been shown that the thermal conductivity in polymers can exhibit significant anisotropy when the polymer chains are partially aligned with each other and this behavior is observed for all kinds of polymer materials, crystalline, semicrystalline, and amorphous.⁶ The anisotropy found in polymers can be related to a statistically averaged orientation of the molecular chains with respect to a reference direction. Hennig⁸ proposed a model that an unoriented polymer is a random aggregate of small fully oriented units. The unit can be either a molecular chain segment called a monomer or a local volumetric unit consisting of aligned molecular chains. They found out that the random orientation of the polymer chains and the weak couplings between the chains are the two main reasons accounted for the experimentally observed low thermal conductivity of polymers. Random orientation of the polymer chains in amorphous polymers can shorten the mean-free path of the phonons,

which are the major energy carriers in polymers, thus rendering the low thermal-conductivity value of polymers. This is then further confirmed with the experiments which shows that the thermal conductivity can be increased when the polymer sample is stretched.⁶

On the other hand, single polymer chain can potentially have much higher thermal conductivity than its bulk counterpart since it is an intrinsically low-dimensional material system.⁹ Theoretical studies of various one-dimensional lattice models suggest that low-dimensional materials can have an very large or even infinite thermal conductivity.¹⁰ Two excellent examples of low-dimensional system are carbon nanotubes and graphene sheets, with room-temperature thermal conductivity of 3000 W/mK and 5000 W/mK,¹¹ respectively. Freeman *et al.*¹² is the one who performed early molecular-dynamics (MD) simulations of thermal conductivity in a fairly realistic polymer chain. They find out that the thermal conductivity of individual chains is higher than the corresponding bulk polymer material. Recently, the simulations by Henry and Chen^{13,14} show that the thermal conductivity of a single polyethylene chain can exceed 100 W/mK if the chain is longer than 40 nm. Their analysis shows that single polyethylene chain can have many times higher thermal conductivity than the bulk polyethylene material.

In short, the thermal conductivity of polymers is not intrinsically low. Single polymer chain which is a low-dimensional material has rather high thermal conductivity. The measured low thermal conductivity of bulk polymers could be attributed to the random orientation and entanglement of polymer chains. If polymer chains could be aligned, one would expect anisotropy and high thermal conductivity of polymers in certain directions. Technically it would be much more favorable to increase thermal conductivity of polymers by aligning polymer chains than adding high thermal-conductivity metallic or ceramic fillers for some applications such as polymer electronics. Several mechanisms could be explored to practically align polymer chains, including mechanical stretching mentioned above, and recently developed molecular layer deposition techniques¹⁵ which can

fabricate polymer thin films with aligned chains. A value of 37.5 W/mK (Ref. 16) has been measured for polyethylene in the stretching direction. When stretching a polymer sample, the draw ratio is defined as the ratio of the final length after stretching to the original length. As draw ratio increases, the thermal conductivity in the stretching direction increases rapidly and a value of 70 W/mK is extrapolated from experiments for polyethylene with fully aligned chain.¹⁷ Recently the thermal conductivity of polyethylene nanofibers has been measured to be as high as ~ 104 W/mK (diameters of 50–500 nm and lengths up to tens of millimeter) under mechanical stretch.¹⁸ Recent simulation results also predict the axial thermal conductivity of a polyethylene crystal with fully aligned chains to be as high as 310 ± 190 W/mK.¹⁹

Though a few experiments and simulations have been done to show the great promise in enhancing the thermal conductivity of polymers, a systematic research is still needed to study the fundamental mechanisms on how mechanical strains can be used to tune the structure and thermal conductivity of polymers. Such studies could play significant roles in the development of polymer electronics and polymer thermal interface materials. In this paper, we conduct stretching deformation and thermal-conductivity simulations using all-atom molecular-dynamics simulation to study the tuning mechanisms of thermal conductivity under mechanical strains. Atomic simulation enables us to correlate the thermal conductivity change with the change in chain conformation under mechanical strains. This study can be used to guide the future development of advanced reconfigurable and tunable thermal management technologies.

II. MODELING AND SIMULATION

In this work, molecular-dynamics simulation is used to study the thermal-conductivity tuning of polymers under mechanical strains. MD simulation is a powerful technique to study the equilibrium and transport properties of polymers, in which the motion of the molecules is treated classically, an approximation that is reasonable for many important problems in polymer materials.^{20–22} Various studies have been carried out on the mechanical properties of polymers under mechanical strains,^{23,24} the chain orientation change due to strains,^{25,26} and the thermal properties of polymers (without strain).^{19,27–29} However, there are very few existing work studying how and why the strain could affect the thermal conductivity of polymers. The most relevant study is a simulation by Lussetti *et al.*,³⁰ who calculated the thermal conductivities of stretched polymer samples in parallel and perpendicular to the stretching directions, which confirms the measured thermal-conductivity anisotropy of polymers under mechanical strain. However, how the chain conformation changes under mechanical strains and could the thermal conductivity change be correlated with the conformation change remain as important fundamental questions if one would explore mechanical strains to tune the thermal conductivity for advanced thermal management technologies. This work is to shed some lights on fundamentals on answering these questions.

Polyethylene is chosen as our model material system to study the strain effects on the thermal conductivity of poly-

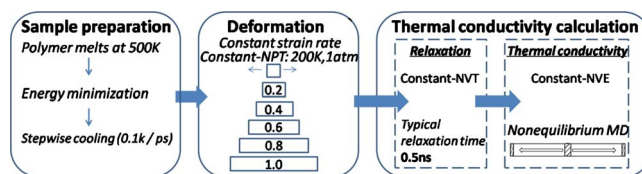


FIG. 1. (Color online) Numerical simulation procedure for building structure-property relationships of polymers when they are under mechanical strains, which involves three major steps: sample preparation, deformation, and thermal-conductivity calculation simulations. After amorphous polymer sample is prepared, the deformation process generates a series of strained samples at different strains, then the thermal conductivity of these strained samples are calculated.

mers due to its simplicity.^{31–33} Polyethylene is a polymer consisting of long chains of ethylene monomers. The all-atom model³⁴ which takes into account all the carbon and hydrogen atoms is adopted in this study and is expected to reveal the atomic details under mechanical strains.²² We note that both Freeman *et al.* and Enrico *et al.* used united-atom model for their studies, which lumps all the hydrogen atoms into the carbon atoms.

Our simulation is conducted in a simulation domain that contains ten randomly coiling polyethylene chains with each chain containing $N=200$ carbon atoms, corresponding to a molecular weight (molar mass) $M=2802$ g/mol. Small N gives a poor representation of bulk behavior. As N becomes larger, we would expect an increasingly better approximation to a dense amorphous system at a significant increase in computational cost. Lavine *et al.*²⁵ calculated the influences of chain length on the polyethylene deformation and their results show that $N=200$ is large enough for representing bulk deformation behavior. We also build a polyethylene sample containing five randomly coiling chains with $N=400$ carbon atoms in each chain with a molecular weight $M=5602$ g/mol to observe whether there is molecular weight dependence. We used COMPASS force field³⁵ for our simulation, which is a general all-atom force field for atomistic simulation of common organic molecules, small inorganic molecules, and polymers. The COMPASS force field is one of the class II force field, which predicts well the conformational energies and vibration frequencies, both closely relevant to thermal properties of polymers. The details of the COMPASS force-field functional form and associated parameters can be found in the Appendix.

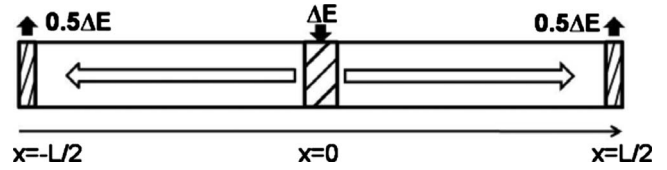
The MD simulations were performed using LAMMPS simulation package.³⁶ All the simulations used 1 fs time step and the force cutoff distance was chosen to be 10 Å. Verlet algorithm was used for the integration of Newton's equations of atomic motion. The neighbor list was checked in every time step. Periodic boundary conditions were applied in all three directions and thus allowing the representation for bulk material. Figure 1 shows the simulation procedure which consists of three modules: sample preparation, deformation (mechanical stretching), and thermal-conductivity simulation. To generate representative glassy polymer sample at low temperature which would be a much easier way to form aligned chain during mechanical straining, we generated

polymer melts at 500 K and then cooled down the polymer melts from 500 to 200 K, which is below the glass transition temperature of polyethylene. Following the procedure in Ref. 37, initial structures of the polymer melts at 500 K were generated using a modified Markov process, based on rotational isomeric state theory and incorporating long-range interactions. Energy minimization was used to relax the samples for 1 ns at 500 K at an applied isotropic pressure of 1 atm. Samples at 200 K were then obtained by stepwise cooling at a rate of 0.1 K/ps to a desired temperature under isotropic controlled pressure conditions followed by subsequent relaxation of 1 ns. 0.1 K/ps cooling rate is chosen based on the simulation results from Lyulin and Michels³⁸ who showed that 0.1 K/ps is slow enough for annealing simulations. In order to eliminate the possible differences brought by initial density, we tested five different initial densities and they all led to the same equilibrium density 0.68 g/cm³, which is reasonable comparing to the experimental density value 0.73 g/cm³ at 1 atm (Ref. 39) because real polyethylene is very difficult to prepare in a completely amorphous state.⁴⁰

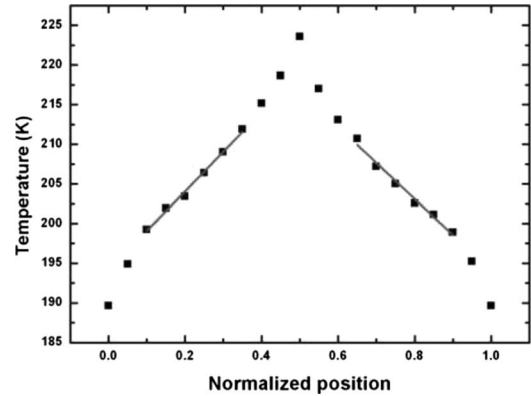
After the sample preparation process, deformation simulations were performed under constant strain-rate condition at 200 K. The constant strain at each time step was applied uniaxially along the x axis of the periodic simulation cell, which is in the same direction as the temperature gradient is applied in later thermal-conductivity simulations. Pressure was kept constant at 1 atm for all other boundaries during deformation, which uses constant-NPT (number of particles, pressure, and temperature) ensemble to adjust the atom positions. Both strain rates of 10^9 and 10^8 s⁻¹ were simulated. We periodically stopped the stretching during the deformation process to generate a series of samples which are under different mechanical strains. Before calculating the thermal conductivity, these strained polymer samples were relaxed until the structures are stable employing constant-NVT (constant number of particles, volume, and temperature) ensemble, which typically takes 0.5 ns for the relaxation. The thermal conductivity was then calculated using the nonequilibrium molecular-dynamics simulation.⁴¹⁻⁴³ This approach relies on imposing a temperature difference across a simulation cell and calculating the resulted heat flux⁴⁴ or imposing a heat flux and calculating the resulted temperature gradient.^{45,46} The thermal conductivity can then be calculated using the Fourier's law of heat conduction, shown in Eq. (1),

$$\mathbf{J} = -\kappa \nabla T, \quad (1)$$

where \mathbf{J} is the local heat flux, κ is the thermal conductivity, and ∇T is the temperature gradient. A schematic representation of the simulation cell used to compute the thermal conductivity κ is shown in Fig. 2(a). The simulation cell which is stretched to a length L is divided into twenty slabs, each with thickness δ . To create a heat flux along the x -axis direction of the simulation cell, which is the same direction of the applied strains, small amount of heat ΔE is added into a thin slab of thickness δ centered at $x=0$ (hot region) at each time step and the same amount of heat is removed from two half slabs of thickness 0.5δ centered at $x=L/2$ and $x=-L/2$ (cold regions). Such heat addition and removal is done through



(a)



(b)

FIG. 2. (a) A schematic representation of the simulation cell used to compute the thermal conductivity and (b) typical temperature profile and linear fitting of nonequilibrium molecular-dynamics simulation for thermal conduction.

velocity rescaling. For consistency, we have checked the dependence of the computed thermal conductivity on the cross-sectional area, heat source/sink width, and the magnitude of the input heat flux and found the dependence on computational variables to be quite weak.⁴⁷ When the system reached steady state, typically after 1.7 ns, the heat flux can be calculated as $J_z = \Delta E / 2A\Delta t$, where A is the cross-sectional area of the simulation domain and Δt is the time step, respectively. To calculate the temperature gradient, the temperature of each slab is averaged over the last 1 ns of the simulations. Figure 2(b) shows a typical temperature profile. We fit only the linear temperature region which is not close to the hot and cold region, as shown in Fig. 2(b), to calculate the thermal conductivity using the Fourier heat conduction equation.

III. RESULTS AND DISCUSSIONS

A. Thermal-conductivity enhancement

Figure 3 shows the thermal conductivity of polyethylene samples stretched at different strains (0–2.0) under different strain rates of 10^8 and 10^9 s⁻¹. The thermal conductivity in the stretching direction of the polymer sample is enhanced with increasing strain for both strain rates. Thermal conductivity perpendicular to the stretching direction decreases with the increasing strain. When the polymer sample is stretched three times of the original length, the thermal conductivity in the stretching direction is enhanced for more than five times. Stretching deformation forces the polymer chains to orient in the stretching direction which induces the chain alignment. Therefore, in a stretched sample, there are more backbone

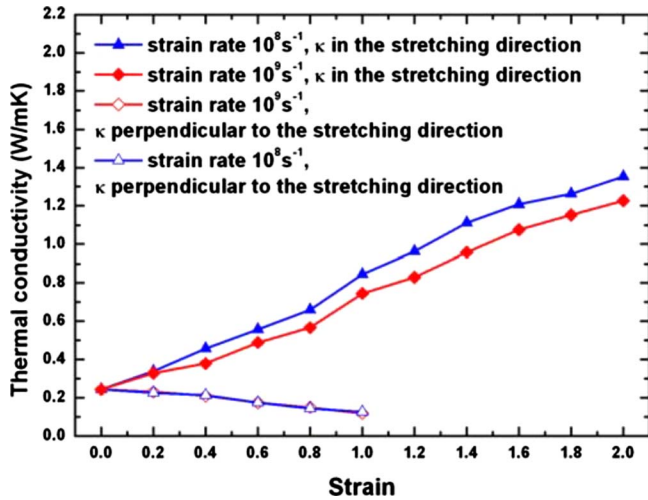


FIG. 3. (Color online) The change in the thermal conductivity of polymers in the stretching direction and perpendicular to the stretching direction as a function of tensile strains. It also shows that the slower the strain rate, the higher the enhancement of the thermal conductivity in the stretching direction.

bonds oriented in the stretching direction than perpendicular to the stretching direction. Thermal energy transports more efficiently along the polymer chain, which consists of the strong carbon-carbon covalent bonds, than perpendicular to the polymer chain. Similar thermal-conductivity enhancement in the stretching direction has been found experimentally.^{16,48–51} High density or ultrahigh molecular weight polyethylene are often used in such stretching experiments. We also found that the enhancement of thermal conductivity in the stretching direction is dependent on the strain rate that the polymer samples are stretched. The slower the sample is stretched, the higher the thermal-conductivity enhancement. Figure 4 shows the dependence of the thermal-conductivity enhancement on molecular weight. The larger the molecular weight, the higher the thermal conductivity

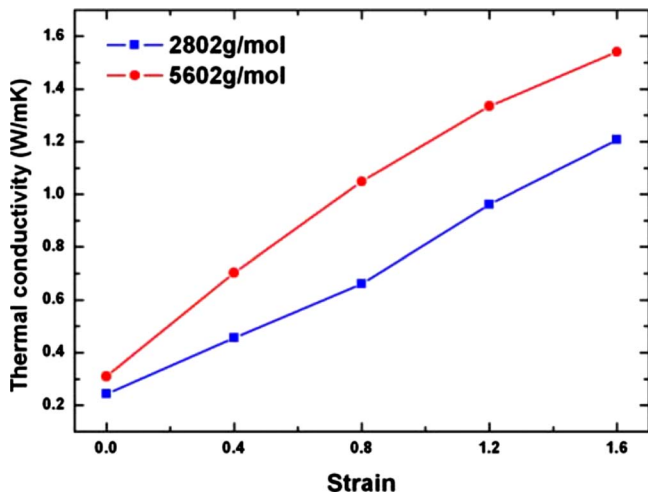


FIG. 4. (Color online) The dependence of the thermal-conductivity enhancement on molecular weight. The larger the molecular weight, the higher the thermal conductivity when the polymer is stretched at the same strain rate of 10^9 s^{-1} to the same strain.

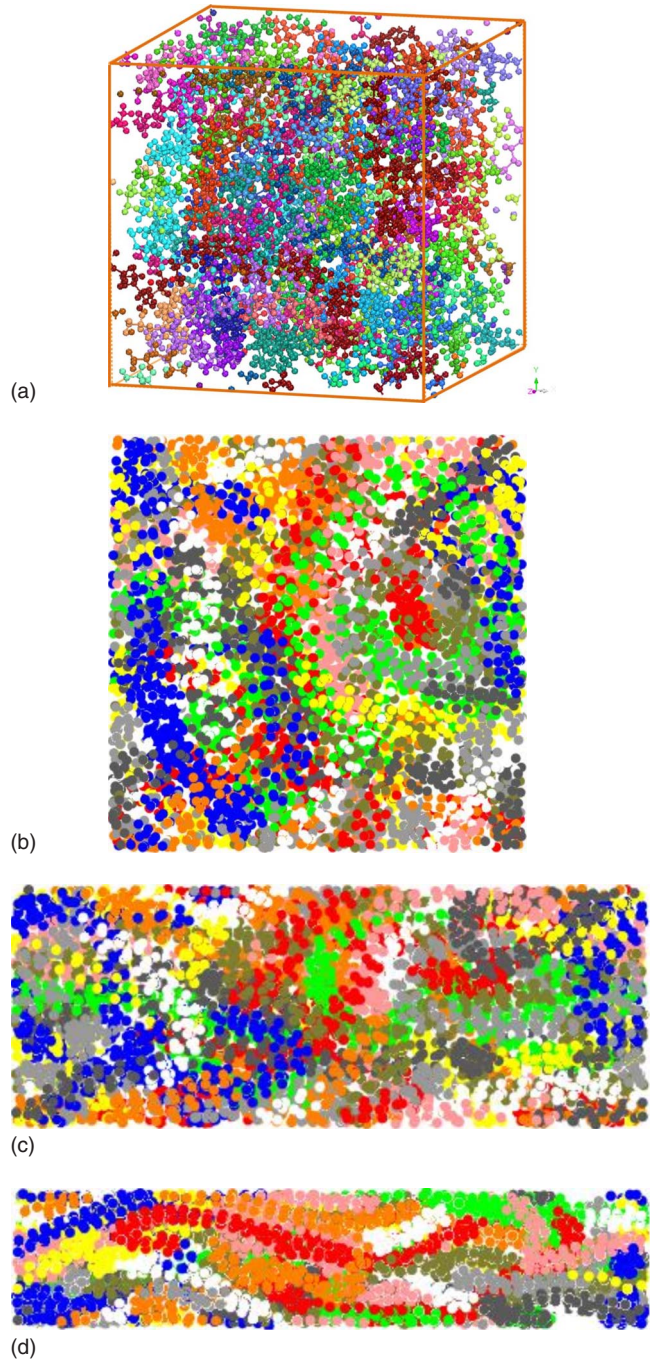


FIG. 5. (Color online) (a) 3D unit cell of the polymer sample under zero strain, (b) projection to XY plane of the samples before deformation, (c) when stretched at $\epsilon=1$ with a strain rate of 10^9 s^{-1} , and (d) when stretched at $\epsilon=2$ with a strain rate 10^9 s^{-1} .

when the polymer is stretched at the same strain rate of 10^9 s^{-1} to the same strain.

B. Chain alignment

In order to understand the strain effects on the polymer chain structures and to develop thermal conductivity-chain orientation relationship, we investigated the chain alignment due to the stretching deformation. Figure 5 shows the chain

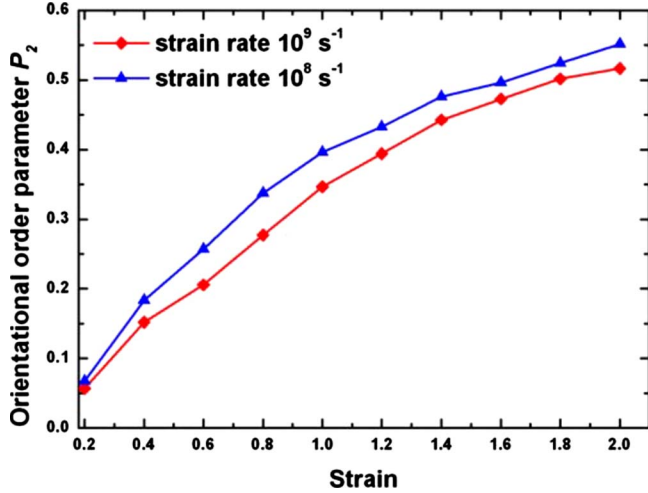


FIG. 6. (Color online) The change in orientational order parameter P_2 as a function of the mechanical strain after relaxation. The orientation will increase mostly at small strains while slow down the increasing rate at relatively larger strains.

alignment visualization figures, plotted using VMD software⁵² and MATERIAL STUDIO software package. In these figures, ten different colors (including the white color) represent ten different polymer chains in a simulation domain. Figure 5(a) shows the three-dimensional (3D) unit cell of the polymer sample before mechanical tuning (stretching deformation). The initial chains are in random coil conformations. To see it more clearly, Figs. 5(b)–5(d) are the XY plane projection of the 3D snapshots of the sample before deformation, stretched at $\varepsilon=1$ and stretched at $\varepsilon=2$ respectively, under the strain rate of 10^9 s^{-1} . Clearly the chains gradually align themselves to the stretching direction.

To quantify the polymer chain alignment, we calculated the orientational order parameter^{23–26,53} which is a useful indicator for chain alignment. The local chain direction at each atom is characterized by the unit vector, which is computed from the chord vectors connected to the atom: $\mathbf{e}_i = (\mathbf{r}_{i+1} - \mathbf{r}_{i-1}) / |\mathbf{r}_{i+1} - \mathbf{r}_{i-1}|$. A chord is defined as a line segment connecting two second-nearest neighbors on the same chain.²⁵ Alignment of chain chord vectors with the applied strain direction or orientational order parameter P_2 is then computed as

$$P_2 = 1.5 \langle (\mathbf{e}_i \cdot \mathbf{e}_x)^2 \rangle - 0.5, \quad (2)$$

where \mathbf{e}_x is the unit vector in the direction of applied strain. The orientational order parameter is sometimes called the Hermans orientation function.⁵⁴ The orientational order parameter for the polymer system is simply the average of the values of each single chain.

We calculated the orientational order parameters of the polymer samples during relaxation after the samples are deformed at different strains. As the relaxation proceeds, the orientational order parameter values decay slightly. Figure 6 plots the averaged orientational order parameters for the last 400 ps during the 0.5 ns relaxation process. The orientational order parameter increases due to the stretching, which means the structure will be more aligned, as visualized in Fig. 5.

Moreover, the orientational order parameter increases mostly at small strains and slows down the increasing rate at relatively larger strains. This is reasonable because the chain-unfolding process largely increases the chain alignment while the chain stretching through monomer rotation improves the chain alignment relatively slowly. When the polymer sample is stretched at a slower rate, there is much more time (ten times more in our case) for the chains to uncoil themselves and for the monomers in the chains to rotate and adjust the positions to reach better alignment. Thus we observed the phenomena that the enhancement of the orientational order parameter is larger when the sample is stretched at slower strain rate. This strain-rate dependence of chain orientation indeed renders us another controlling parameter to tune the thermal conductivity with mechanical strain, agreeing well with the observations of the strain-rate-dependent thermal conductivity in Fig. 3.

C. Thermal conductivity-orientational order parameter relationship

Figures 3 and 6 in the previous sections show that the thermal conductivity and the orientational order parameter have similar enhancement trends with the applied mechanical strains. The reason is that mechanical strain induces the chain conformation change in order to align polymer chains to the stretching direction. Heat transport is more efficient along aligned chain structures than through randomly coiled structures. In addition, the enhancement of both the thermal conductivity and the orientational order parameter is larger when the sample is stretched at slower strain rate.

There should be direct relationship between the thermal conductivity and the orientational order parameter. In Fig. 7, we plotted the thermal conductivity versus the orientational order parameter for two strain rates and two molecular weights and found the exponential curve $\kappa = \kappa_0 \exp(aP_2)$ fits the relationship very well. The fitting parameters are shown in Table I. Hennig⁸ predicts a linear relation between the thermal resistivity and P_2 using series thermal resistance model, which assumes that the total thermal resistance of the material is given by the series of the thermal resistances of the individual units. Their analytical approach gives lower bound of the thermal conductivity and does not reflect the detailed molecular nature of polymers. Our molecular-dynamics simulation reflects the structural evolution of polymer material polyethylene when under applied strain. P_2 is then calculated based on structure details in the molecular level. We have thus predicted an exponential dependence of thermal conductivity with P_2 , different from Hennig's analytical model. The reason for the exponential dependence is explained as follows. When P_2 is small, which means some

TABLE I. The fitting parameters for κ - P_2 relationship.

	κ_0	a
Strain rate 10^9 s^{-1} , $M=2802 \text{ g/mol}$	0.27547	2.82401
Strain rate 10^8 s^{-1} , $M=2802 \text{ g/mol}$	0.27968	2.83779
Strain rate 10^9 s^{-1} , $M=5602 \text{ g/mol}$	0.25655	2.94617

TABLE II. Force-field parameters for our simulation (Ref. 35). (A) Bond length [$E=K_2(b-b_0)^2+K_3(b-b_0)^3+K_4(b-b_0)^4$]. (B) Bond angle [$E=K_2(\theta-\theta_0)^2+K_3(\theta-\theta_0)^3+K_4(\theta-\theta_0)^4$]. (C) Torsion angle [$E=K_1(1-\cos\Phi)+K_2(1-\cos 2\Phi)+K_3(1-\cos 3\Phi)$]. (D) van der Waals interaction ($E=\varepsilon[2(r^*/r)^9-3(r^*/r)^6]$). (E) Bond increment ($E=332q_iq_j/r_{ij}$, where $q_i=\sum_k\delta_{ik}$). (F) Bond/bond [$E=K(b-b_0)(b'-b'_0)$]. (G) Bond/angle [$E=K(b-b_0)(\theta-\theta_0)$]. (H) Angle/angle [$E=K(\theta-\theta_0)(\theta'-\theta'_0)$]. (I) Angle/angle/torsion [$E=K(\theta-\theta_0)(\theta'-\theta'_0)\cos\Phi$]. (J) Bond/torsion (central bond) [$E=(b-b_0)[K_1(1-\cos\Phi)+K_2(1-\cos 2\Phi)+K_3(1-\cos 3\Phi)]$]. (K) Bond/torsion (terminal bond) [$E=(b'-b'_0)[K_1(1-\cos\Phi)+K_2(1-\cos 2\Phi)+K_3(1-\cos 3\Phi)]$]. (L) Angle/torsion [$E=(\theta-\theta_0)[K_1(1-\cos\Phi)+K_2(1-\cos 2\Phi)+K_3(1-\cos 3\Phi)]$].

Bond	b_0 (Å)	K_2 (kcal mol ⁻¹ Å ⁻²)	K_3 (kcal mol ⁻¹ Å ⁻³)	K_4 (kcal mol ⁻¹ Å ⁻⁴)	
H-C	1.1010	345.0000	-691.8900	844.6000	
C-C	1.5300	299.6700	-501.7700	679.8100	
Angle	θ_0 (deg)	K_2 (kcal mol ⁻¹ rad ⁻²)	K_3 (kcal mol ⁻¹ rad ⁻³)	K_4 (kcal mol ⁻¹ rad ⁻⁴)	
H-C-H	107.6600	39.6410	-12.9210	-2.4318	
H-C-C	110.7700	41.4530	-10.6040	5.1290	
C-C-C	112.6700	39.5160	-7.4430	-9.5583	
Torsion	K_1 (kcal mol ⁻¹)	K_2 (kcal mol ⁻¹)	K_3 (kcal mol ⁻¹)		
H-C-C-H	-0.1432	0.0617	-0.1530		
H-C-C-C	0.0000	0.0316	-0.1681		
C-C-C-C	0.0000	0.0514	-0.1430		
Atom	r_i^* (Å)	ε_i (kcal mol ⁻¹)			
C	3.8540	0.0620			
H	2.8780	0.0230			
Bond		$\delta_{ik}(e)$			
H-C		-0.0530			
C-C		0.0000			
Bond/bond		K (kcal mol ⁻¹ Å ⁻²)			
H-C/H-C		3.3872			
H-C/C-C		5.3316			
C-C/C-C		0.0000			
Bond/angle	K (kcal mol ⁻¹ Å ⁻¹ rad ⁻²)	Bond/angle	K (kcal mol ⁻¹ Å ⁻¹ rad ⁻²)		
H-C/H-C-H	18.1030	C-C/H-C-C	20.7540		
H-C/H-C-C	11.4210	C-C/C-C-C	8.0160		
Angle/angle	Common bond	K (kcal mol ⁻¹ rad ⁻²)	Angle/angle	Common bond	K (kcal mol ⁻¹ rad ⁻²)
H-C-H/H-C-H	H-C	-0.3157	H-C-C/H-C-C	C-C	-0.4825
H-C-H/H-C-C	H-C	0.2738	H-C-C/C-C-C	C-C	-1.3199

TABLE II. (Continued.)

Bond	b_0 (Å)	K_2 (kcal mol ⁻¹ Å ⁻²)	K_3 (kcal mol ⁻¹ Å ⁻³)	K_4 (kcal mol ⁻¹ Å ⁻⁴)	
H-C-C/H-C-C	H-C	0.1184	C-C-C/C-C-C	C-C	-0.1729
Angle/angle/ torsion			K (kcal mol ⁻¹ rad ⁻²)		
H-C-C/ H-C-C/ H-C-C-H			-12.5640		
H-C-C/ C-C-C/ H-C-C-C			-16.1640		
C-C-C/C-C-C/ C-C-C-C			-22.0450		
Bond/torsion	K_1 (kcal mol ⁻¹ Å ⁻¹)	K_2 (kcal mol ⁻¹ Å ⁻¹)	K_3 (kcal mol ⁻¹ Å ⁻¹)		
C-C/H-C-C-H	-14.2610	-0.5322	-0.4864		
C-C/H-C-C-C	-14.8790	-3.6581	-0.3138		
C-C/C-C-C-C	-17.7870	-7.1877	0.0000		
Bond/torsion	K_1 (kcal mol ⁻¹ Å ⁻¹)	K_2 (kcal mol ⁻¹ Å ⁻¹)	K_3 (kcal mol ⁻¹ Å ⁻¹)		
H-C/H-C-C-H	0.2130	0.3120	0.0777		
H-C/H-C-C-C	0.0814	0.0591	0.2219		
C-C/H-C-C-C	0.2486	0.2422	-0.0925		
C-C/C-C-C-C	-0.0732	0.0000	0.0000		
Angle/torsion	K_1 (kcal mol ⁻¹ rad ⁻¹)	K_2 (kcal mol ⁻¹ rad ⁻¹)	K_4 (kcal mol ⁻¹ rad ⁻⁴)		
H-C-C/ H-C-C-H	-0.8085	0.5569	-0.2466		
H-C-C/ H-C-C-C	0.3113	0.4516	-0.1988		
C-C-C/ H-C-C-C	-0.2454	0.0000	-0.1136		
C-C-C/ C-C-C-C	0.3886	-0.3139	0.1389		

of the chains are still folded or coiled, heat transport is limited by the folded or even entangled regions. However, as the P_2 improves, the chains gradually unfold themselves and stretch out along the stretching direction. Then heat transport through aligned structure is preferred and a little improvement in chain alignment will result in relatively larger improvement in heat transport.

It is interesting to take a closer look to the two parameters in the fitting formula, which are helpful to predict the material property. K_0 represents thermal conductivity of isotropic polymer material, which can be also seen from the formula when P_2 is zero. We obtained $K_0=0.275$ W/mK for $P_2=0$ which is comparable to the literature value 0.20–0.25 W/mK

for isotropic low-density amorphous polyethylene.^{7,55} The parameter a represents how fast the thermal conductivity increases with the orientational order parameter. If we extrapolate the thermal conductivity in our simulation for $P_2=1$, we obtained a value of 4.64 W/mK for perfect polymer with molar mass of 2800 g/mol. Ni *et al.*¹⁹ performed a molecular-dynamics simulation on perfect aligned polymers and predicted a thermal conductivity of 11.7 W/mK. Considering the possible differences that could be from the different force fields used for simulations and the defects (voids) might be involved in our bulk material simulation, we believe our results are consistent with Ni *et al.* Moreover, the close value of the exponential fitting parameters for both

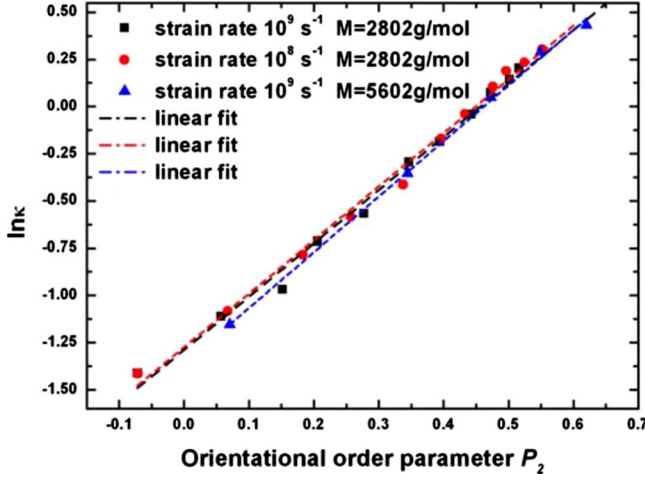


FIG. 7. (Color online) The relationship between the logarithm of the enhanced thermal conductivity and the orientational order parameter P_2 using linear fit.

strain rates manifests that the thermal conductivity is only determined by the orientational order parameter. Strain-rate differences could result in thermal-conductivity difference but are well captured by the orientational order parameter.

It is worthwhile to discuss the dependence of thermal conductivity on molecular weight. In our simulation, we find that the dependence of the thermal conductivity on molecular weight of polyethylene at the same strain rate and constant P_2 is different. Figure 4 shows that higher thermal conductivity is obtained for polymers with higher molecular weight when stretched at the same strain rate 10^9 s^{-1} to the same strain. Figure 7 shows that smaller thermal conductivity is obtained for polymers with larger molecular weight at constant P_2 within our calculation range. By calculating the thermal conductivity of crystalline polyethylene with perfectly aligned chains ($P_2=1$) along the polymer chains for different molar mass (molecular weight), Ni *et al.*¹⁹ find that the calculated thermal conductivity increase monotonically as the molecular weight of the polymer increases. Both Ni *et al.*¹⁹ and Henry and co-workers^{14,18} explained the dependence on molecular weight by viewing the polymer chain ends as chain defects, which prevent the effective heat transport in the perfectly aligned chain polymer. Apparently we find a different trend for the dependence of thermal conductivity on molecular weight for amorphous polymers than the work by Ni *et al.* and Henry *et al.* in perfectly aligned polymers due to the chain entanglements in the polymers.

IV. CONCLUSIONS

The low thermal conductivity of polymers limits their heat spreading capability, which is one of the major technical barriers for the polymer-based products, especially electronics, such as organic light emitting diodes. Mechanical

stretching could align the polymer chains and enhance the thermal conductivity. All-atom model molecular-dynamics simulation has been conducted to study the tuning of polymer thermal conductivity using mechanical strains. The simulation results show that both the thermal conductivity of polymers and the orientational order parameter, which is a quantitatively indicator of the chain conformations and alignments, increases with the increasing strain. Strain rate is another controlling parameter to tune the thermal conductivity with mechanical strain. The enhancements of the thermal conductivity and the orientational order parameter are larger under the same strain when the polymer is stretched slower. Molecular weight also has influence on the thermal conductivity of strained polymers. Finally, we related the thermal conductivity with the orientational order parameter through an exponential relation. This structure-property relationship can guide us on tuning the thermal conductivity of polymers with the mechanical strains.

ACKNOWLEDGMENTS

The authors would like to thank Kurt Maute for the help on computational resources. This work is supported by AFOSR/DCT under Grant No. FA9550-08-1-0078 and NSF under Grant No. CMMI 0729520.

APPENDIX: FUNCTIONAL FORM AND ASSOCIATED PARAMETERS OF COMPASS FORCE FIELD

The force-field functional form used in this simulation is shown in Eq. (A1),³⁵

$$\begin{aligned}
 E_{total} = & \sum_b [k_2(b - b_0)^2 + k_3(b - b_0)^3 + k_4(b - b_0)^4] \\
 & + \sum_\theta [k_2(\theta - \theta_0)^2 + k_3(\theta - \theta_0)^3 + k_4(\theta - \theta_0)^4] \\
 & + \sum_\phi [k_1(1 - \cos \phi) + k_2(1 - \cos 2\phi) \\
 & + k_3(1 - \cos 3\phi)] + \sum_\chi k_2\chi^2 + \sum_{b,b'} k(b - b_0)(b' - b'_0) \\
 & + \sum_{b,\theta} k(b - b_0)(\theta - \theta_0) + \sum_{b,\phi} (b - b_0)[k_1 \cos \phi \\
 & + k_2 \cos 2\phi + k_3 \cos 3\phi] + \sum_{\theta,\phi} (\theta - \theta_0)[k_1 \cos \phi \\
 & + k_2 \cos 2\phi + k_3 \cos 3\phi] + \sum_{b,\theta} k(\theta' - \theta'_0)(\theta - \theta_0) \\
 & + \sum_{\theta,\theta,\phi} k(\theta' - \theta'_0)(\theta - \theta_0)\cos \phi \sum_{i,j} \frac{q_i q_j}{r_{ij}} \\
 & + \sum_{i,j} \epsilon_{ij} \left[2 \left(\frac{r_{ij}^0}{r_{ij}} \right)^9 - 3 \left(\frac{r_{ij}^0}{r_{ij}} \right)^6 \right]. \tag{A1}
 \end{aligned}$$

The functions could be divided into two categories: (1) valence terms including diagonal and off-diagonal cross-coupling terms and (2) nonbonded interaction terms. The valence terms represent internal coordinates of bond, angle,

torsion angle, and out-of-plane angle, and the cross-coupling terms include combinations of two or three internal coordinates. The cross-coupling terms are important for predicting vibration frequencies and structural variations associated with the conformational changes. All the force-field param-

eters used in our simulation can be found in Table II. According to our system, the atom types for carbon and hydrogen atoms are c4 and h1 in COMPASS force field, which represent generic carbon and nonpolar hydrogen, respectively.

*ronggui.yang@colorado.edu

- ¹C. Liu, *Adv. Mater.* **19**, 3783 (2007).
- ²G. Maier, *Mater. Today* **4**, 22 (2001).
- ³T. Shimoda, M. Kimura, S. Miyashita, R. H. Friend, J. H. Burroughes, and C. R. Towns, *SID Int. Symp. Digest Tech. Papers* **30**, 372 (1999).
- ⁴W. U. Huynh, J. J. Dittmer, and A. P. Alivisatos, *Science* **295**, 2425 (2002).
- ⁵B. Scrosati, F. Croce, and S. Panero, *J. Power Sources* **100**, 93 (2001).
- ⁶K. Kurabayashi, *Int. J. Thermophys.* **22**, 277 (2001).
- ⁷D. J. David, *Relating Materials Properties to Structure: Handbook and Software for Polymer Calculations and Materials Properties* (Technomic, PA, 1999).
- ⁸J. Hennig, *J. Polym. Sci. Part C: Polym. Symp.* **16**, 2751 (1967).
- ⁹S. Lepri, R. Livi, and A. Politi, *Phys. Rep.* **377**, 1 (2003).
- ¹⁰E. Fermi, J. Pasta, and S. Ulam, *E. Fermi Collected Papers* (University of Chicago Press, Chicago, 1965), Vol. 2, p. 978.
- ¹¹A. A. Balandin, S. Ghosh, W. Bao, I. Calizo, D. Teweldebrhan, F. Miao, and C. N. Lau, *Nano Lett.* **8**, 902 (2008).
- ¹²J. J. Freeman, G. J. Morgan, and C. A. Cullen, *Phys. Rev. B* **35**, 7627 (1987).
- ¹³A. Henry and G. Chen, *Phys. Rev. B* **79**, 144305 (2009).
- ¹⁴A. Henry and G. Chen, *Phys. Rev. Lett.* **101**, 235502 (2008).
- ¹⁵N. M. Adamczyk, A. A. Dameron, and S. M. George, *Langmuir* **24**, 2081 (2008).
- ¹⁶C. L. Choy, Y. W. Wong, G. W. Yang, and T. Kanamoto, *J. Polym. Sci., Part B: Polym. Phys.* **37**, 3359 (1999).
- ¹⁷M. Pietralla, *J. Comput.-Aided Mater. Des.* **3**, 273 (1996).
- ¹⁸S. Shen, A. Henry, J. Tong, R. Zheng, and G. Chen, *Nat. Nanotechnol.* **5**, 251 (2010).
- ¹⁹B. Ni, T. Watanabe, and R. P. Simon, *J. Phys.: Condens. Matter* **21**, 084219 (2009).
- ²⁰K. Binder, J. Horbach, W. Kob, W. Paul, and F. Varnik, *J. Phys.: Condens. Matter* **16**, S429 (2004).
- ²¹W. G. Sawyer, S. S. Perry, S. R. Phillpot, and S. B. Sinnott, *J. Phys.: Condens. Matter* **20**, 354012 (2008).
- ²²S. J. Heo, I. Jang, P. R. Barry, S. R. Phillpot, S. S. Perry, W. G. Sawyer, and S. B. Sinnott, *J. Appl. Phys.* **103**, 083502 (2008).
- ²³N. M. Lavecic, R. S. Maxwell, A. Saab, and R. H. Gee, *J. Phys. Chem. B* **110**, 3588 (2006).
- ²⁴M. Roberge, R. E. Prud'homme, and J. Brisson, *Polymer* **45**, 1401 (2004).
- ²⁵M. S. Lavine, N. Waheed, and G. C. Rutledge, *Polymer* **44**, 1771 (2003).
- ²⁶P. Gestoso and J. Brisson, *J. Polym. Sci., Part B: Polym. Phys.* **40**, 1601 (2002).
- ²⁷T. Terao, E. Lussetti, and F. Muller-Plathe, *Phys. Rev. E* **75**, 057701 (2007).
- ²⁸A. Henry and G. Chen, *Nanoscale Microscale Thermophys. Eng.* **13**, 99 (2009).
- ²⁹K. Fukui, B. G. Sumpter, M. D. Barnes, D. W. Noid, and J. U. Otaigbe, *Macromol. Theory Simul.* **8**, 38 (1999).
- ³⁰E. Lussetti, T. Terao, and F. Muller-Plathe, *J. Phys. Chem. B* **111**, 11516 (2007).
- ³¹B. Monasse, S. Queyroy, and O. Lhost, *Int. J. Mater. Form.* **1**, 1111 (2008).
- ³²D. J. Lacks and G. C. Rutledge, *J. Phys. Chem.* **98**, 1222 (1994).
- ³³M. S. Al-Haik and M. Y. Hussaini, *Mol. Simul.* **32**, 601 (2006).
- ³⁴A. S. Henry and G. Chen, *J. Comput. Theor. Nanosci.* **5**, 141 (2008).
- ³⁵H. Sun, *J. Phys. Chem. B* **102**, 7338 (1998).
- ³⁶S. Plimpton, *J. Comput. Phys.* **117**, 1 (1995).
- ³⁷D. N. Theodorou and U. W. Suter, *Macromolecules* **18**, 1467 (1985).
- ³⁸A. V. Lyulin and M. A. J. Michels, *Phys. Rev. Lett.* **99**, 085504 (2007).
- ³⁹M. J. Richardson, P. J. Flory, and J. B. Jackson, *Polymer* **4**, 221 (1963).
- ⁴⁰D. Brown and J. H. R. Clarke, *Macromolecules* **24**, 2075 (1991).
- ⁴¹C. Oligschleger and J. C. Schon, *Phys. Rev. B* **59**, 4125 (1999).
- ⁴²P. K. Schelling, S. R. Phillpot, and P. Keblinski, *Phys. Rev. B* **65**, 144306 (2002).
- ⁴³P. K. Schelling, S. R. Phillpot, and P. Keblinski, *J. Appl. Phys.* **95**, 6082 (2004).
- ⁴⁴J. R. Lukes, D. Y. Li, X. G. Liang, and C. L. Tien, *J. Heat Transfer* **122**, 536 (2000).
- ⁴⁵F. Müller-Plathe, *J. Chem. Phys.* **106**, 6082 (1997).
- ⁴⁶P. Jund and R. Jullien, *Phys. Rev. B* **59**, 13707 (1999).
- ⁴⁷X. W. Zhou, S. Aubry, R. E. Jones, A. Greenstein, and P. K. Schelling, *Phys. Rev. B* **79**, 115201 (2009).
- ⁴⁸C. L. Choy, W. H. Luk, and F. C. Chen, *Polymer* **19**, 155 (1978).
- ⁴⁹D. T. Morelli, J. Heremans, M. Sakamoto, and C. Uher, *Phys. Rev. Lett.* **57**, 869 (1986).
- ⁵⁰L. Piraux, M. Kinany-Alaoui, J. P. Issi, D. Begin, and D. Billaud, *Solid State Commun.* **70**, 427 (1989).
- ⁵¹D. B. Mergenthaler, M. Pietralla, S. Roy, and H. G. Kilian, *Macromolecules* **25**, 3500 (1992).
- ⁵²W. Humphrey, A. Dalke, and K. Schulten, *J. Mol. Graphics* **14**, 33 (1996).
- ⁵³C. W. Yong and P. G. Higgs, *Macromolecules* **32**, 5062 (1999).
- ⁵⁴D. I. Bower, *An Introduction to Polymer Physics* (Cambridge University Press, New York, 2002).
- ⁵⁵C. L. Choy, *Polymer* **18**, 984 (1977).